The *kakapo* Mutation Affects Terminal Arborization and Central Dendritic Sprouting of *Drosophila* Motorneurons

Andreas Prokop,* Jay Uhler,* John Roote,‡ and Michael Bate*

*Department of Zoology and ‡Department of Genetics, University of Cambridge, Cambridge CB2 3EH, United Kingdom

Abstract. The lethal mutation *l(2)CA4* causes specific defects in local growth of neuronal processes. We uncovered four alleles of *l(2)CA4* and mapped it to bands 50A-C on the polytene chromosomes and found it to be allelic to *kakapo* (Prout et al. 1997. *Genetics.* 146:275–285). In embryos carrying our *kakapo* mutant alleles, motorneurons form correct nerve branches, showing that long distance growth of neuronal processes is unaffected. However, neuromuscular junctions (NMJs) fail to form normal local arbors on their target muscles and are significantly reduced in size. In agreement with this finding, antibodies against kakapo (Gregory and Brown. 1998. *J. Cell Biol.* 143:1271–1282) detect a specific epitope at all or most *Drosophila* NMJs. Within the central nervous system of *kakapo* mutant embryos, neuronal dendrites of the RP3 motorneuron form at correct positions, but are significantly reduced in size. At the subcellular level we demonstrate two phenotypes potentially responsible for the defects in neuronal branching: first, transmembrane proteins, which can play important roles in neuronal growth regulation, are incorrectly localized along neuronal processes. Second, microtubules play an important role in neuronal growth, and *kakapo* appears to be required for their organization in certain ectodermal cells: On the one hand, *kakapo* mutant embryos exhibit impaired microtubule organization within epidermal cells leading to detachment of muscles from the cuticle. On the other, a specific type of sensory neuron (scolopidial neurons) shows defects in microtubule organization and detaches from its support cells.

Key words: dendrites • *Drosophila* • microtubules • neuromuscular junction • cytoskeleton

THE ability to form synaptic contacts is a fundamental property of developing neurons. To build a neural network, neurons send out processes in a regulated manner, initially by long-distance growth into defined target areas, followed by recognition and contact of target cells within that region. This final growth phase is characterized by local sprouting of neurites in the target areas and terminal arborization on the surface of target cells, and appears to require mechanisms different from those underlying long distance growth (Caroni, 1997). Although it is well established that the development of neuronal circuits depends on a sequence of precisely regulated growth events, the underlying mechanisms are still poorly understood.

Neurite growth is carried out by specialized structures, growth cones, that are formed either at the distal end of the neurite or by budding off from already established axons. Growth cones respond to diffusible and contact-mediated signals in their environment, which can be attractive or repulsive, pulling and pushing the growth cone along its path (Tessier-Lavigne and Goodman, 1996). Such extrinsic information can be used not only for guidance of growth cones, but also to change and regulate their growth behavior. For example, in vertebrates, agrin released from muscles downregulates long-distance growth of incoming growth cones and upregulates their ability to form terminal branches and to differentiate synapses (Ruegg and Bixby, 1998). Furthermore, neuronal growth is regulated by intrinsic properties of the growing neuron. For example, in crayfish different motorneuronal terminals arborize in the absence of target muscles in culture, and the degree to which they arborize is neuron-specific and reminiscent of their growth behavior in vivo (Arcaro and Lnenicka, 1995). Similar intrinsic determination of the size of neuronal terminals has been demonstrated in vivo for sensory neurons of crickets or *Drosophila* (Murphey and Lemere, 1984; Canal et al., 1998). Also in vertebrates, graft experiments suggest that certain growth properties, such as the length to which axons extend, can be crucially dependent on intrinsic cues (Caroni, 1997). Thus, neuronal growth is regulated by a combination of extrinsic signals and intrinsic properties of the growing neuron.

Address correspondence to A. Prokop, Institut für Genetik, Zellbiologie, Universität Mainz, Becherweg 32, D-55128 Mainz, Germany. Tel.: (49) 6131-394328 or 393293. Fax: (49) 6131-395845. E-mail: prokop@goofy.zdv.uni-mainz.de

Migrating growth cones extend filopodia which are filled with actin bundles, and distinct changes in the actin cytoskeleton cause newly assembling microtubules to accumulate at the base of these filopodia, consolidating a new part of the axon or dendrite (Bentley and O'Connor, 1994; Smith, 1994). The molecular machinery which intrinsically regulates these events comprises (*a*) the cytoskeletal components tubulin and actin, (*b*) components associating with these cytoskeletal components, e.g., microtubule-associated proteins, (*c*) transmembrane molecules involved in adhesion and signaling, (*d*) components of second messenger pathways, e.g., Gap-43 and Cap-23, Cdc42, Rac, Rho, and (*e*) proteins involved in anterograde and retrograde transport such as nonmuscle myosin or the product of the *Drosophila glued* gene (Landmesser et al., 1990; Avila et al., 1994; Nobes and Hall, 1995; Caroni, 1997; Reddy et al., 1997; Suter and Forscher, 1998). Insights into the function of some of these components give first explanations for how neuronal growth can be regulated and subdivided into different growth phases. For example, repressing *tau* function (a microtubule-associated protein) suppresses the formation of axons (Caceres et al., 1992) whereas MAP2 (another microtubule-associated protein) or CAP-23 and GAP-43 proteins appear to function specifically in local sprouting events but not in long-distance growth (Caceres et al., 1991; Dinsmore and Solomon, 1991; Caroni, 1997).

Here we report the isolation and phenotypic characterization of a paralytic mutation in *Drosophila*, *l(2)CA4*, which affects local neuronal growth. *l(2)CA4* turned out to be allelic to *kakapo* (*kak*; Prout et al., 1997). The *kak* mutation affects terminal branch formation of embryonic motorneurons on muscle surfaces and local sprouting of their dendrites in the central nervous system (CNS).[1] However, long-distance growth of axons appears unaffected in *kak* mutant embryos. We demonstrate that *kak* is required for (*a*) the restricted localization of membrane proteins along axons and (*b*) for the organization of the microtubule cytoskeleton in scolopidial sensory neurons and epidermal cells. Loss of these types of function could account for *kak* mutant phenotypes in local neuronal growth. The phenotypes reported here are in good agreement with the finding that *kak* encodes a potential actin binding cytoskeletal element (Gregory and Brown, 1998; Strumpf and Volk, 1998).

Materials and Methods

Fly Stocks and Genetic Mapping of kak

The *kakapo* (*kak*) alleles kak^{91K}, kak^{el3}, kak^{HG25}, and kak^{SF20} were discovered as second-site lethals on chromosomes isolated from four independent ethylmethane sulfonate (EMS) mutagenesis experiments which were designed to recover new lethal and visible mutations in the *Adh* region. kak^{el3} was found on the $elbow^{3}$ chromosome (Ashburner et al., 1980), kak^{SF20} on $wingblister^{SF20}$ (Ashburner et al., 1980), kak^{91k} on $l(2)35Fc^{91k}$ (Ashburner, M., and J. Roote, unpublished data), and kak^{HG25} was isolated in a screen for new alleles of *wingblister* in which mutagenized chromosomes were screened over $wingblister^{SF20}$ (Ashburner, M., and J. Roote, unpublished data). The gene responsible for this unmapped lethality was designated *l(2)CA4* and now named *kakapo*.

Meiotic mapping using the multiple-marked chromosome *al dp b pr c px sp* located *kak* 17.5 map U to the right of *pr*, 20 map U to the left of *px*, and 1.5 map U on either side of *c* (data not shown) i.e., on chromosome arm 2R, within bands 50–53 of the polytene chromosomes. This location was confirmed and refined when it was discovered that the *kak* alleles were lethal with *Df(2R)CX1* [Df(2R)49D1; 50D1] and *Df(2R)MK1* [Df(2R)50B3-5; 50D1-4; Strumpf and Volk, 1998] but not *Df(2R)50C-38* [Df(2R)50C; 50D] or *Df(2R)50C-101* [Df(2R)50C; 50D; Preston et al., 1996], *Df(2R)vg-B* [Df(2R)49D3-4; 49F15-50A3], *Df(2R)vg-C* [Df(2R)49A4-13; 49E7-F1] or *Df(2R)vg-D* [Df(2R)49C1-2; 49E2-6]. The haplo-lethal deletion segregant from the transposition *Tp(2;3)6r35* [Tp(2;3)50A1-15; 50E1-50F9; 84D1-84D14; Eberl et al., 1989], i.e., *Df(2R)6r35* [Df(2R)50A1-15; 50E1-50F9], does not complement *kak* and shows the typical *kak* mutant neuromuscular and muscle phenotypes in embryos when heterozygous with *kak* alleles. The duplication segregant from *Tp(2;3)6r35*, *Dp(2;3)6r35* [Dp(2;3)50A1-15; 50E1-50F9; 84D1-14] is homozygous lethal but, in heterozygosis, completely rescues the lethality and phenotype of *kak* transheterozygotes, e.g., kak^{el3}/kak^{SF20}; *Dp(2;3)6r35* flies are viable and phenotypically wild-type. Taken together, these data place the *kak* locus in the interval 50A to 50C.

Immunohistochemical Methods

Antibody stainings were carried out using standard techniques (Prokop et al., 1996), at stage 16 on whole mounts and at stage 17 on embryos dissected flat with the help of histoacryl glue (Braun, Melsungen, Germany). At stages 16 and 17, mutant embryos were identified with the help of *CyO* balancer chromosomes expressing *lacZ*, at stage 17 also by paralysis and the typical muscle detachment phenotype. $FasII^{eb112}$ mutant embryos were identified by lack of anti–FasII staining. Embryos carrying four copies of *kak* were collected from a $y;Dp(2;3)6r35/TM6,y^{+}$ strain and identified by their yellow mouthhooks.

As antibody probes we used anti–FasII 1D4 2F3 (mouse monoclonal; 1:20) (Van Vactor et al., 1993), anti–Fas III (mouse monoclonal; 1:4) (Halpern et al., 1991); anti-cysteine string protein (mouse polyclonal; 1:10) (Zinsmaier et al., 1994), anti-synaptotagmin (rabbit polyclonal; 1:1,000) (Littleton et al., 1993), anti–α-adaptin (rabbit polyclonal; 1:200) (González-Gaitán and Jäckle, 1997), and 22C10 (mouse monoclonal; 1:10) (Fujita et al., 1982). For stainings with anti-kakapo antibody (rabbit polyclonal; 1:20) (Gregory and Brown, 1998) flat dissected embryos were fixed for 2 min in 0.25% glutaraldehyde and mildly blocked for 10 min in 10% calf serum in phosphate-buffered saline containing 0.1% Triton-X 100.

Stage 16 embryos were either transferred to araldite and sucked as whole mounts into borosilicate capillaries (Hilgenberg, Malsfeld, Germany) (Prokop and Technau, 1993), or they were transferred to 70% glycerol and dissected flat thereafter. Stage 17 flat preparations were dehydrated and covered with araldite, cut off the glass with a razor blade splinter, and then the mount was embedded under a coverslip. Images were scanned directly from the microscope via a video camera (Kontron Elektronik ProgRes 3012; Eching/Munich, Germany). For clarity, different focal planes were combined into one picture using Photoshop 4.0 software (Adobe Systems, Mountain View, CA). The significance of measurements was tested with a nonparametric Mann-Whitney-U test using StatView software. Neuropile and fascicle areas (see Fig. 5, *A* and *B*) were measured on scanned drawings using the Histogram function within the Photoshop 4.0 software.

DiI Labeling and Analysis

Stage 16 embryos were dissected on poly-L-lysine–coated coverslips and stage 17 embryos were dissected flat on a layer of Sylgard (Dow Corning Corp., Midland, MI) using Histoacryl glue (Braun, Melsungen, Germany) (Broadie and Bate, 1993). DiI labeling was carried out as described elsewhere (Landgraf et al., 1997). In brief, embryos were treated with 0.2 mg/ml collagenase IV (Sigma Chemical Co., St. Louis, MO) in saline for 1.5 min, rinsed with saline, fixed with 3.7% formaldehyde in saline for 2.5 min, and then rinsed with saline once more. DiI (Molecular Probes, Eugene, OR) was dissolved in vegetable oil and backfilled into sharpened glass capillaries which were then bevelled. A small droplet of DiI was deposited on the cleft between muscle VL3/4 (muscle nomenclature according to Bate, 1993) and left to diffuse overnight at 4°C. Labeled neurons were then either photoconverted or were scanned at 0.5-μm steps on a Bio-Rad 1024 confocal microscope (Hercules, CA). Confocal images were projected and analyzed using NIH image (Bethesda, MD). Tracings of

1. *Abbreviations used in this paper:* CNS, central nervous system; Fas, fasciclin; *kak*, *kakapo* gene; MAP, microtubule-associated protein; NMJ, neuromuscular junction.

photoconverted preparations were made using a Zeiss Axiophot (Carl Zeiss Inc., Thornwood, NY) attached to a video monitor and data analyzed with a two-sample, unpaired *t* test using Minitab software (Coventry, UK).

Electrophysiology

Whole-cell recordings of muscles VL3/4 in wild-type and *kak* mutant embryos at late stage 17 were made using standard patch-clamp techniques and solutions (Broadie and Bate, 1993). Muscles were voltage-clamped at −60 mV. Signals were amplified using an Axopatch-1D amplifier (Axon Instruments, Foster City, CA), filtered at 2 or 10 KHz and analyzed using Axotape software (Axon Instruments). Series resistance was 16–22 MOhm, electrode resistance was ~5 MOhm, and capacitance was 18–27 pF.

Electron Microscopy

Ultrastructural analyses were carried out as described previously (Prokop et al., 1996, 1998). In brief, embryos were injected with 5% glutaraldehyde in 0.05 M phosphate buffer, pH 7.2, the injected specimens were cut open at their tips with a razor blade splinter, postfixed for 30–60 min in 2.5% glutaraldehyde in 0.05 M phosphate buffer, briefly washed in 0.05 M phosphate buffer, fixed for 1 h in aqueous 1% osmium solution, briefly washed in dH_2O, treated en bloc with an aqueous 2% solution of uranyl acetate for 30 min, dehydrated, and then transferred to araldite. Serial sections of 30–50 nm (silver-grey) thickness were transferred to formvar-covered carbon-coated slot grids, poststained with lead citrate for 5–10 min, and then examined on a JEOL 200CX (Peabody, MA) or Hitachi H600 (Tokyo, Japan). Transverse serial thin sections were taken ~10–15 μm behind the anterior border of the denticle belts, which can be visualized in semithin sections with the light microscope.

Results

The kak Mutant Alleles Affect Size and Shape of Neuromuscular Junctions, but Neuromuscular Synapses Can Form

We uncovered four lethal alleles of the gene *l(2)CA4* as second-site lethals from four independent EMS mutageneses and mapped them genetically to the cytological location 50A-C on the right arm of chromosome 2 (Materials and Methods). In subsequent complementation tests our *l(2)CA4* alleles failed to complement the lethal phenotype of $kakapo^{V168}$ and $kakapo^{l(2)k03405}$ mutant fly strains (Gregory and Brown, 1998), demonstrating that *l(2)CA4* belongs to the *kakapo* (*kak*) complementation group (Prout et al., 1997). All four alleles (kak^{91k}, kak^{el3}, kak^{HG25}, and kak^{SF20}) are embryonic lethals, they fail to complement each other, and show a paralytic phenotype when homozygous, transheterozygous or hemizygous over deficiencies (Materials and Methods). Paralysis might be caused by dysfunction or developmental defects in the nervous system or in the musculature. In *kakapo* mutant embryos we find defects in both tissues: muscles detach from the epidermis in all alleles (see later), and we consistently find a reduction in the size of motorneuronal terminals on muscles and of neuronal branches in the CNS at late stage 17.

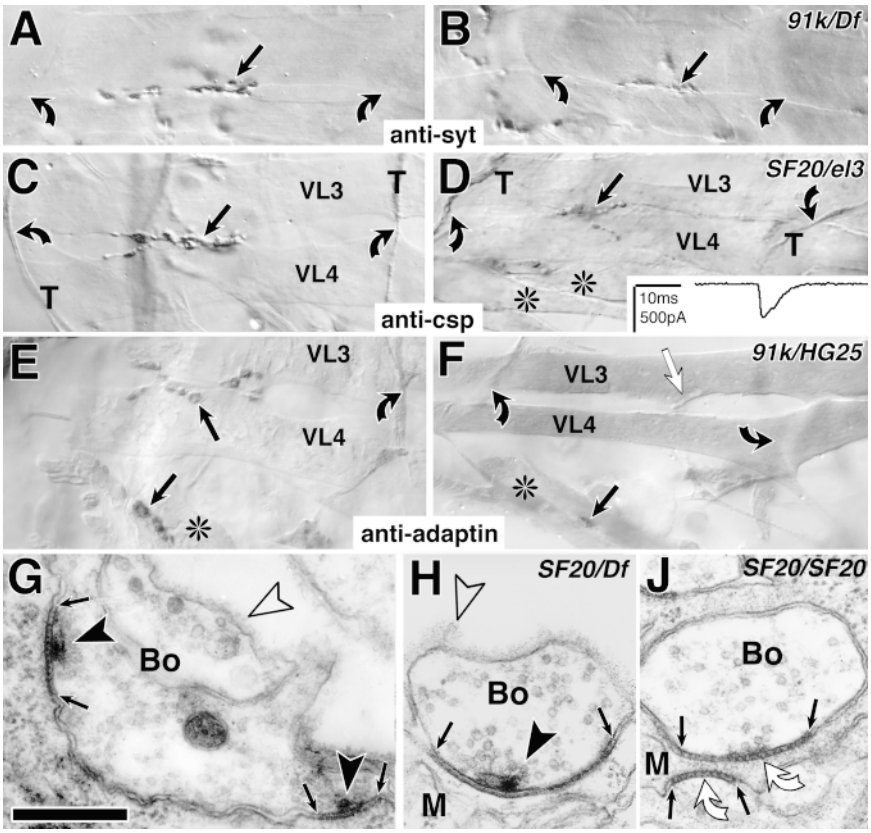

Figure 1. *kak* mutant NMJs are reduced in size at stage 17. (*A–F*) Light microscopic view of NMJs (*black arrows*) on ventral longitudinal muscles VL3 and 4 (nomenclature as in Bate, 1993) or ventral oblique muscles (*) in the central abdomen (A3 to 5) of control (*left*) and *kak* mutant embryos (*right*; allelic combination indicated top right corner) labeled with anti-synaptotagmin (*anti-syt* in *A* and *B*), anti-cysteine string protein (*anti-csp* in *C* and *D*), or anti–α-adaptin (*E* and *F*; control and mutants were stained together in each case); muscle tips (*bent arrows*), in *C* and *D* also indicated by csp-labeled transverse nerve (*T*). *kak* mutant NMJs are reduced in size (*right*), but synaptic transmission occurs (*D*, *inset*, electrophysiological trace recorded from the muscle in *D*). (*F*) In kak^{91k}/kak^{HG25} mutant embryos NMJs are extremely reduced (*black arrow*) and often synaptic markers fail to detect them, although the incoming nerve can be seen (*white arrow*). (*G–J*) Ultrastructure of control (*G*) and *kak* mutant embryos (*H* and *J*). *kak* mutant NMJs exhibit junctions between nerve terminal (*Bo*) and muscle (*M*), and synapses with regularly structured material in the synaptic cleft (between *small arrows*), T-shaped dense bars (*black arrowheads*), and clustered vesicles (*H*). Occasionally T-bars are missing (*J*). *Open arrowheads*, basement membrane. Bars: (*A–F*) 9 μm; (*G–J*) 300 nm.

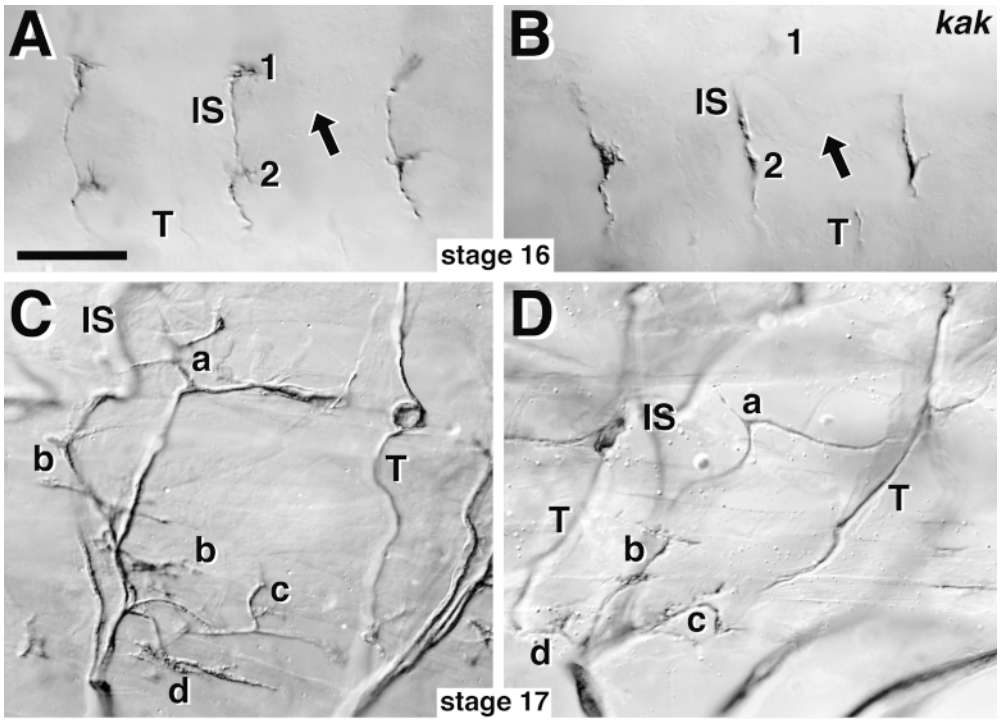

Figure 2. Nerve branches can form and be maintained in *kak* mutant embryos. Control embryos on the left, kak^{el3}/kak^{SF20} mutant embryos on the right, anterior is to the left and dorsal up, all preparations are labeled with anti–Fas II antibodies. (*A*) Three segments in dorsolateral view at stage 16 with the dorsal tips of transverse nerves (*T*) and intersegmental nerves (*IS*), which form NMJs on muscles DA1/DO1 (*1*) and DA2/DO2 (*2*; muscle nomenclature according to Bate, 1993). *Arrows*, dorsoventral position of the trachea. (*B*) In *kak* mutant embryos intersegmental and transverse nerves reach their target area. (*C* and *D*) At stage 17 all segmental nerve branches (*a–d*, Thomas et al., 1984) can be identified in *kak* mutant embryos, but are mislocated, most likely secondarily due to the muscle detachment phenotype (Fig. 6). Bar, 30 μm.

We first describe the neuromuscular junction (NMJ) phenotype. In wild-type embryos at stage 17, motorneuronal terminals have branches on their target muscles with varicosities (boutons) of up to 1 μm in diameter (Broadie and Bate, 1993; Yoshihara et al., 1997). We visualized boutons with antibodies raised against synaptotagmin, cysteine string protein, or α-adaptin, proteins involved in fusion or recycling of synaptic vesicles (Fig. 1, *A*, *C*, and *E*) (Littleton et al., 1993; Zinsmaier et al., 1994; González-Gaitán and Jäckle, 1997). In *kak* mutant embryos NMJs in all locations occupy far less surface of their respective muscles, their branches are reduced in length, and boutons appear reduced in number and size (tested allelic combinations: *SF20/SF20*, *el3/el3*, *91k/91k*, *SF20/el3*, *SF20/91k*, *91k/HG25*, *SF20/Df(2R)6r35*, *SF20/Df(2R)MK1*, *el3/Df(2R)-6r35*, *el3/Df(2R)CX1*, *91k/Df(2R)MK1*, *HG25/Df(2R)-MK1*). Whereas some allelic combinations exhibit an almost complete absence of NMJs (Fig. 1 *F*), other combinations show less severe phenotypes (Fig. 1, *B* and *D*), but their phenotype is nevertheless significant (e.g., relation of NMJ length to muscle length on muscles VL3 and 4 in central abdominal segments is 44 ± 8% in controls, n = 18, and 28 ± 10% in *SF20/91k*, *SF20/el3*, and *el3/Df(2R)-6r35*, n = 38; P = 0.0001). Although NMJs are severely reduced in *kak* mutant embryos, presynaptic marker expression is mainly restricted to neuromuscular sites (for example Fig. 1 *F*) and can hardly be found in ectopic locations (in contrast to other classes of mutant embryos; Prokop et al., 1996). This reduced and restricted appearance of synaptic markers in *kak* mutant embryos hints at a requirement for *kak* within the presynaptic terminal (see Discussion).

Ultrastructural analyses of *kak* mutant embryos reveal that presynaptic boutons can form normal cell junctions with the muscle, interspersed by morphologically normal synapses (Fig. 1 *H*; for details of wild-type NMJs see Fig. 1 *G*) (Broadie et al., 1995; Prokop et al., 1996). However, we found examples where synapses were indicated by structured material in the neuromuscular cleft, but typical presynaptic specializations (T-bars) were missing (Fig. 1 *J*). If T-bars were found, they were restricted to neuromuscular sites, corroborating our light microscopic findings. Furthermore, neuromuscular contacts and synapses were found less frequently compared with controls, which is in agreement with the reduction of NMJs observed at the light microscopic level. To test whether transmission occurs at *kak* mutant NMJs we carried out patch recordings on kak^{SF20}/kak^{el3} mutant muscles. These recordings revealed excitatory junctional currents, clearly indicating that neuromuscular transmission occurs (Broadie and Bate, 1993). In four cases we stained the NMJs with antibodies raised against cysteine string protein subsequent to recording (Fig. 1 *D*) and confirmed that in all cases the NMJ was clearly misshapen and reduced in size. Occurrence of neuromuscular transmission is furthermore demonstrated by the presence of strong muscle contractions in *kak* mutant embryos observed under polarized light in vivo.

Taken together, ultrastructural, electrophysiological and in vivo observations suggest that NMJs, although abnormal in shape, are functional in *kak* mutant embryos.

This suggests that *kak* might be required specifically for growth and shaping of branches at motorneuronal terminals.

kak Function Appears To Be Required for Local, but Not Long-distance Growth

The reduction of NMJ size could be the result of a general inhibition or delay of axonal growth. To test this idea we used the axonal markers anti–Fasciclin II (Fas II) and Fasciclin III (Fas III) to analyze the peripheral branching pattern of motor axons during stage 16, when these axons have just reached their target muscles in the wild type (Fig. 2) (Halpern et al., 1991; Van Vactor et al., 1993): peripheral nerves can form correctly in *kak* mutant embryos (tested combinations: *SF20/el3*, *91k/HG25*, *SF20/Df(2R)-MK1*). Only the short SNb-branch has a tendency to stall at the entry point into the ventral muscle field, as observed by SNb-specific Fas III staining in kak^{91k}/kak^{HG25} and $kak^{SF20}/Df(2R)MK1$ mutant embryos at early stage 16 (data not shown). However, as the longest nerves (SNa and ISN) reach their target areas in *kak* mutant embryos there is no indication of general impairment of neuronal growth (Fig. 2 *B*). At stage 17 the peripheral nerve pattern has become distorted in *kak* mutant embryos due to muscle detachment (see below). However, in interpretable cases, anti–Fas II stainings reveal a normal pattern of nerve branches (Fig. 2 *D*).

Thus, in *kak* mutant embryos motorneurons appear capable of navigating along correct paths to their target muscles and maintaining these contacts thereafter. This suggests that our *kak* mutant alleles affect NMJ formation during the differentiation phase, when muscle-attached growth cones reshape into the branches and boutons of mature NMJs (Broadie and Bate, 1993; Yoshihara et al., 1997).

kak Protein Is Expressed at NMJs

To investigate whether *kak* function might be required directly within the nerve terminal, we used an anti-kak antiserum (Gregory and Brown, 1998). Our staining procedure (Materials and Methods) failed to detect strong staining at NMJs in wild type or hemizygous embryos, however, in *Dp(2;3)6r35* embryos NMJs are labeled more reliably and strongly (Fig. 3, compare *A* and *C* with *B*). *Dp(2;3)6r35* embryos carry four copies of *kak* due to a duplication of a chromosomal region involving *kak* (Materials and Methods), suggesting that the enhanced immunoreactivity at the NMJ is specific for kak. Also at late larval stages anti-kak antibodies label spots of up to 2 μm at the NMJ, which by size appear to be presynaptic boutons (Fig. 3 *D*).

kak Mutations Affect Dendritic Growth of RP3 Motorneurons in the CNS

Local neuronal growth is not restricted to branch formation at the NMJ but also occurs within the CNS during the development of dendritic branches at stage 16/17. We tested whether this growth might also be affected in *kak* mutant embryos. We labeled dendrites retrogradely by applying DiI to the NMJ of RP3 motorneurons on muscles VL3/4 (Landgraf et al., 1997). In wild-type embryos, RP3 sends an axon contralaterally through the dorsally located anterior root of the intersegmental nerve. On the ipsilateral side a second projection leaves the soma of RP3, projecting along a similar path as the contralateral process,

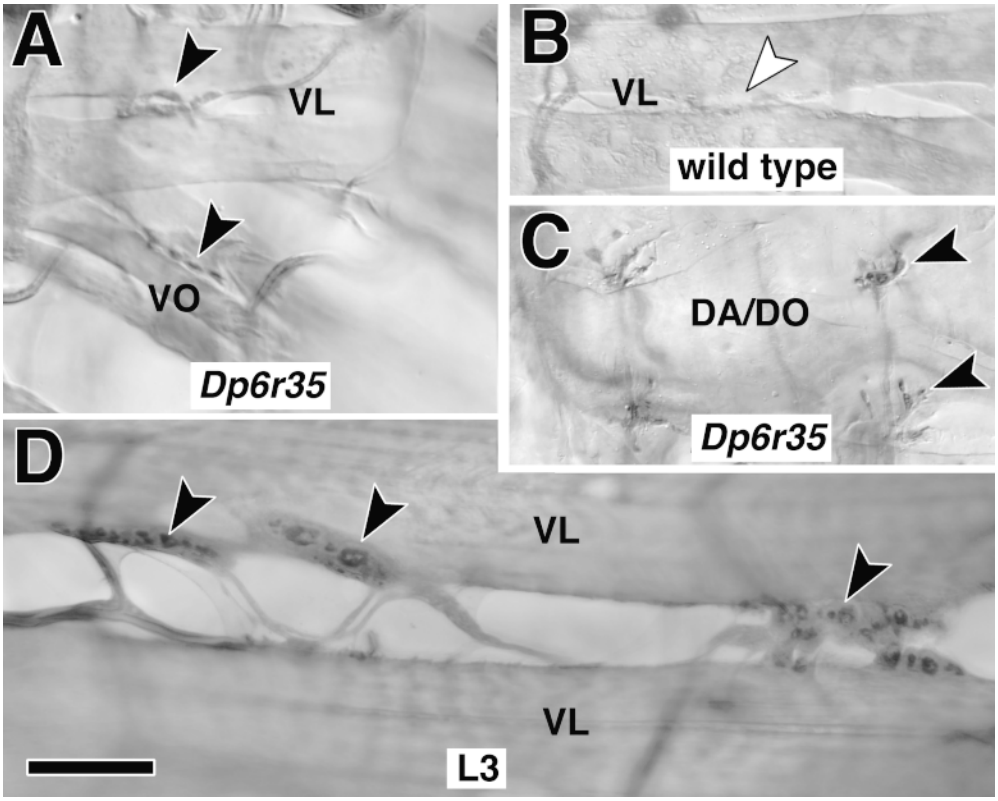

Figure 3. kakapo is localized at NMJs. (*A–C*) At stage 17 anti-kakapo staining is found at NMJs (*arrowheads*; shown NMJs are on ventral longitudinal [*VL*], ventral oblique [*VO*], and dorsal acute and oblique muscles [*DA/DO*]; muscle nomenclature according to Bate, 1993). In embryos carrying four copies of *kak* (indicated as *Dp6r35*) anti-kak staining is stronger and more reliable than in embryos carrying one (data not shown) or two copies (*wild type*) of *kak* (compare *black arrowheads* in *A* and *C* with *white arrowhead* in *B*; *A* and *B* were dissected and processed in the same drop of solution). (*D*) At the late larval NMJ (L3) kakapo staining appears concentrated in the presynaptic boutons (*black arrowheads*). Bar, 9 μm.

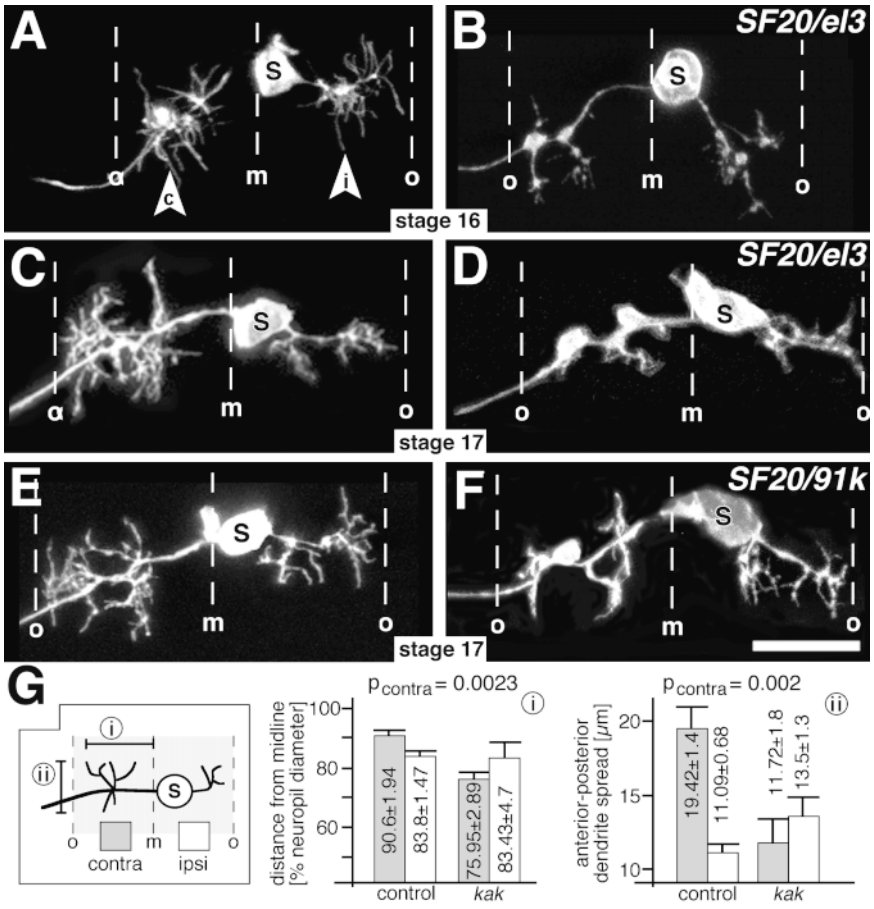

Figure 4. Central dendrites are affected in *kak* mutant embryos. (*A–F*) DiI-labeled RP3 neurons in control (*left*) and *kak* mutant embryos (*right*; allelic combination indicated top right corner) at late stage 16 (*A* and *B*) or stage 17 (*C–F*). Anterior is up in all panels. Midline (*m*) and outer neuropile borders (*o*) are indicated. The soma (*S*) of RP3 lies close to the midline sending an ipsilateral process (*i* in *arrowhead*) and a contralateral axon (*c* in *arrowhead*), both of which have extensive dendritic arborizations. Branching of dendrites is affected mainly on the contralateral side of *kak* mutant embryos from stage 16 onwards. Note that the somata of *kak* mutant RP3 neurons appear malformed. (*G*) Schematic presentation of the modes (box on *left*) and results (*i* and *ii*) of measurements: mediolateral spread of dendrites measured from the midline (*i*) and their largest spread in anterior-posterior direction (*ii*) show significant differences on the contralateral side (*grey columns*, contralateral; *white columns*, ipsilateral; p_{contra}, significance for contralateral measurements). Bar, 10 μm.

but remaining confined to the neuropile. Both projections have numerous local arborizations (Fig. 4, *C* and *E*) (Landgraf et al., 1997; Sink and Whitington, 1991). In kak^{SF20}/kak^{el3} and in kak^{SF20}/kak^{91k} mutant embryos the ipsilateral local arborizations are almost normal, but the contralateral arborizations are severely reduced and often form swellings or blobs (Fig. 4, *D* and *F*). We quantified the spread of the dendritic arborization by measuring either the longest distance of dendrites from the midline in the mediolateral axis, or the maximal spread of dendrites in the anterior-posterior axis. With both methods only the spread of the contralateral dendritic arbor is significantly reduced in *kak* mutant embryos whereas the spread of the ipsilateral side is similar to wild type (Fig. 4 *G*). The failure of RP3 to elaborate its contralateral dendrites is apparent from late stage 16 (Fig. 4, compare *A* with *B*), suggesting *kak* function to be required for the process of outgrowth rather than maintenance of dendrites. As in *kak* mutant embryos, the contralateral arborizations of RP3 form within the correct region of the neuropile (*kak*: 37–76% of the mediolateral neuropile diameter; controls: 24–91%) they might reach their correct target areas, as similarly observed for their neuromuscular projections.

Consistent with the findings for the RP3 dendrites, the whole neuropile is reduced in size in *kak* mutant embryos compared with wild type, but appears normal in its organization. In transverse sections of anti–Fas II–labeled nerve cords at stage 17 the neuropile area is reduced to 73% ($P = 0.0084$) in kak^{SF20}/kak^{el3} mutant embryos, but the number and position of Fas II–positive longitudinal fascicles is normal (for details see Fig. 5, *A* and *B*). However, measurements of midline-associated fascicles (Fig. 5, *A* and *B*, *M1* and *M2*) reveal a significant reduction to 50% of wild-type size ($n = 17$ for *kak* and 22 for wild type; $P = 0.0001$). Taken together, our findings suggest that neurons project correctly, but fail to elaborate part of their local branches, leading to smaller NMJs in the periphery and smaller dendrites and thus reduced neuropile volume centrally.

kak Function Is Required To Regulate the Localization of Membrane Proteins within Neuronal Processes

The phenotypes shown so far strongly suggest a specific requirement for *kak* function in specific local growth events. In the following we describe further *kak* mutant phenotypes, i.e., mislocalization of axonal proteins and disorganization of the cytoskeleton, both of which are potential causes underlying the specific defects in neuronal branch formation.

First, we observed a mislocalization of proteins along neuronal processes. For example, Fas II, which encodes a transmembrane protein of the immunoglobulin superfamily (Goodman and Doe, 1993), is expressed at low levels in the nerve roots and stops at the entry point into the neuro-

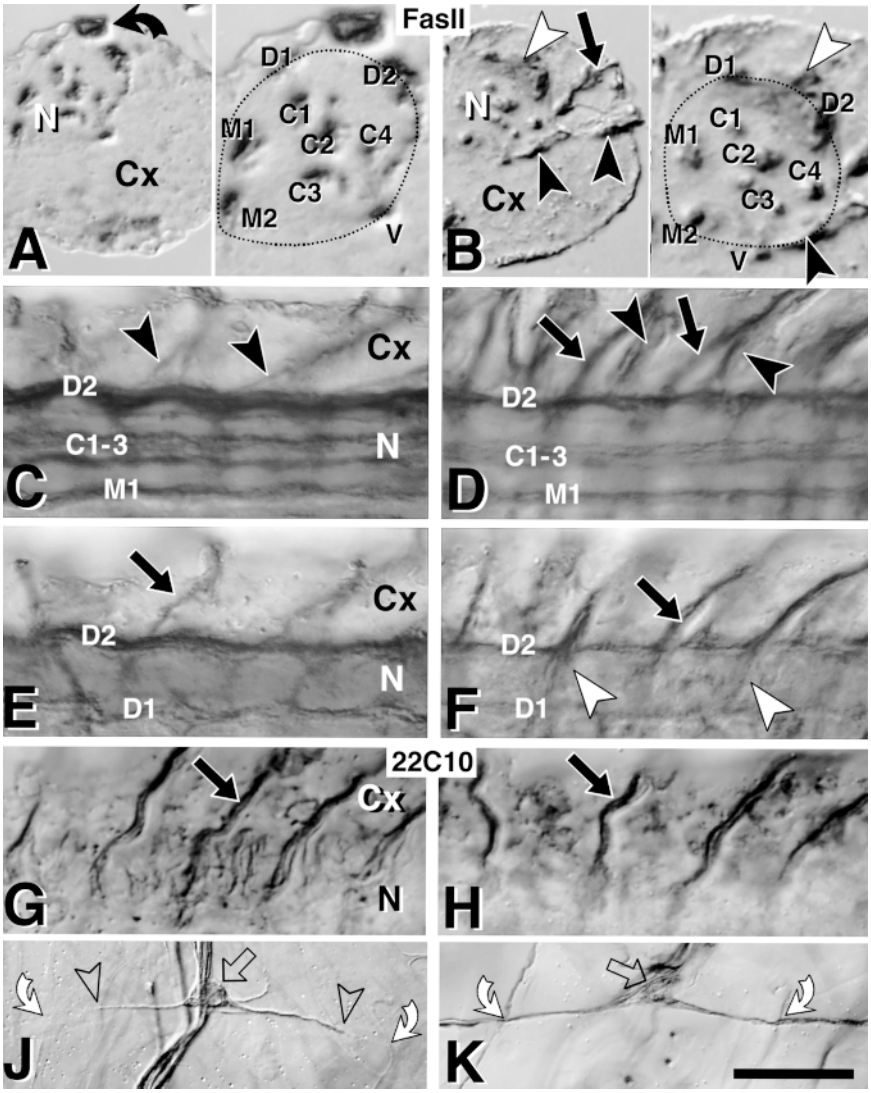

Figure 5. Axonal markers are misexpressed in *kak* mutant embryos. All nerve cords are late stage 17, control embryos on the left, kak^{el3}/kak^{SF20} mutant embryos on the right. (*A*) Right half of a transverse section through a Fas II–labeled ventral nerve cord (*Cx*, cortex; *N*, neuropile; *bent arrow*, β-Gal labeled cell due to blue balancer), and a close-up of the neuropile on the right (*stippled line*). Dorsal (*D1* and *D2*), ventral (*V*), median (*M1* and *M2*), and central (*C1–C4*) Fas II–positive longitudinal fascicles are indicated. (*B*) In *kak* mutant nerve cords all longitudinal fascicles are present but partly reduced in size (*M1* + *M2* in *B* reduced to 70% compared with *A*), as is the whole neuropile (*stippled area*; *B/A* = 80%). The split into subfascicles seen in C3 occurs similarly in fascicles C1, 2 and 3 also in wild type (data not shown). Nerve roots strongly express FasII only in the mutant (*black* and *white arrowheads*; *black arrow* in *B*). (*C–H*) Dorsal views of the right half of ventral nerve cords (3–4 hemisegments shown; anterior to the left; *C* and *D* are more ventral, *E–H* are more dorsal) stained with anti–Fas II (*C–F*) or 22C10 (*G* and *H*); symbols correspond to those in *A* and *B*. Ventral (*black arrowheads*; only shown for Fas II) and dorsal (*black arrows*) nerve roots in the mutant embryos (*right*) stain more strongly for Fas II but with similar strength for 22C10, when compared with control embryos (*left*). (*J*) Processes of the dorsal bipolar dendrite neurons of the peripheral nervous system (*open arrows*, cell bodies) span a whole epidermal segment (*bent arrows*, crossing points with transverse nerve at segment border), but 22C10 expression is restricted to the proximal part (between *open arrowheads*). (*K*) In *kak* mutant embryos 22C10 extends along the entire process. Note that the profile of soma and dendrites is less sharp and more irregular than in the control. Bars: (*A–H*) 18 μm; (*J* and *K*) 40 μm.

pile of stage 16 and 17 control embryos (Fig. 5, *C* and *E*). Fas II expression in kak^{SF20}/kak^{el3} and kak^{91k}/kak^{HG25} mutant nerve cords exhibits no obvious differences at stage 16 (data not shown), but by stage 17 Fas II expression in all nerve roots is strongly upregulated and the anterior root of the intersegmental nerve extends to the dorsal part of the neuropile (Fig. 5, *B*, *D*, and *F*). This phenotype at late stage 17 was confirmed using other allelic combinations of *kak* (*el3/Df(2R)CX1*, *SF20/SF20*, *SF20/91k*; *91k/HG25*) (data not shown). Thus, it appears as if Fas II fails to localize properly along neuronal processes. In contrast, 22C10 immunoreactivity, which detects membrane-associated or transmembrane proteins (Angaut-Petit et al., 1998), appears to be distributed normally in *kak* mutant nerve roots (Fig. 5, compare *G* with *H*), but we found a mislocalization phenotype in another type of neuron, the dorsal bipolar neuron of the peripheral nervous system. The dorsal bipolar neurons have longitudinal projections that span the entire length of the segment (Bodmer and Jan, 1987), but only the proximal regions of these processes are labeled by 22C10 antibodies in the wild type (Fig. 5 *J*). However, in kak^{SF20}/kak^{el3}, kak^{SF20}/kak^{91k}, and kak^{91k}/kak^{HG25} mutant embryos the entire length of these lateral bipolar projections is 22C10-positive (Fig. 5, *K*). Thus, *kak* function is required for the correct localization of (membrane) proteins within neuronal processes, and the mislocalization of such proteins is a potential cause for defects in local branching in the neuropile or at the NMJ (Suter and Forscher, 1998) (see Discussion).

The Microtubule Cytoskeleton Is Affected in kak Mutant Embryos

Neuronal growth requires a dynamic cytoskeleton (Bentley and O'Connor, 1994; Suter and Forscher, 1998). Some *kak* mutant phenotypes suggest that *kak* function might be

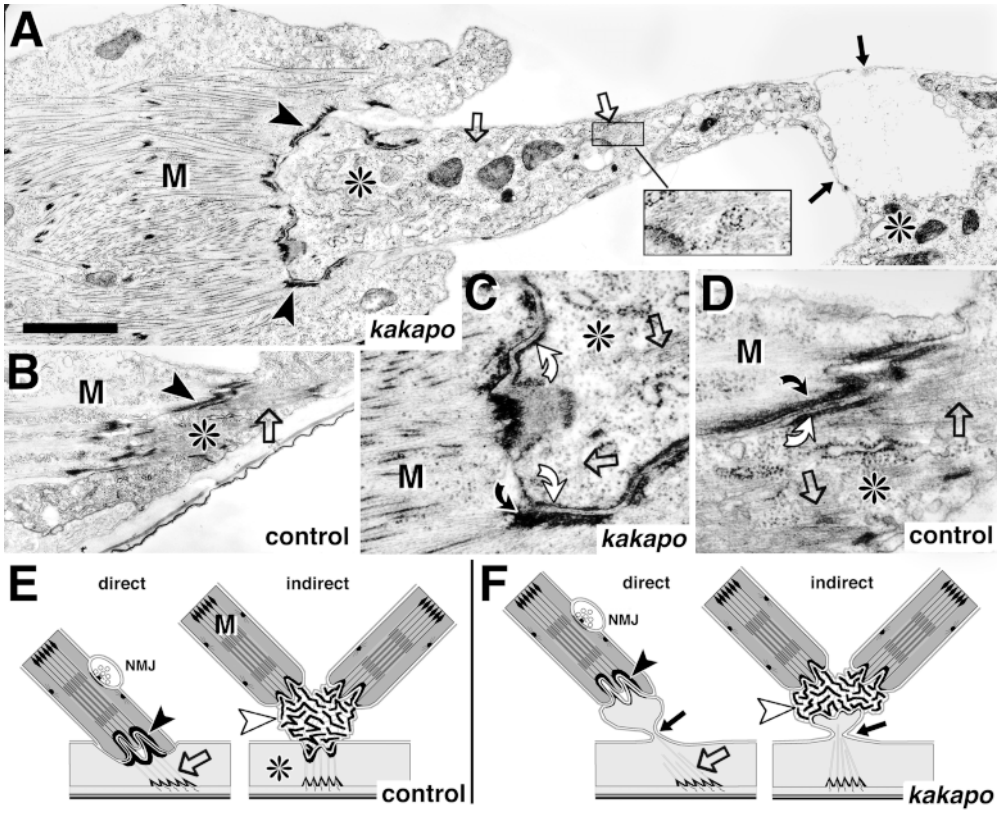

Figure 6. At muscle attachment sites *kak* mediates anchoring of microtubules to the membrane. (*A–D*) Direct muscle attachment sites at stage 17 in *kakapo* mutant (*A* and *C*) and wild-type embryos (*B* and *D*; genotypes indicated at bottom right corner). Muscles (*M*) and epidermal cells (*) are closely apposed at connecting hemiadherens junctions in control and mutant embryos (*C* and *D* and *arrowheads* in *A* and *B*), but the epidermal cells rupture in the mutant embryos (*black arrows* in *A* and *F*). (*C* and *D*) At the hemiadherens junctions membrane-associated material in the muscle (*bent black arrows*) anchors thin filaments in control and mutant embryos. Similar dense material in the epidermal cell (*bent white arrows*) anchors microtubules (*open arrows*) in control embryos, but fails to do so in *kak* mutant embryos, in spite of the presence of microtubules (*open arrow*s in *A* and *C*; *inset* in *A*). The schematic representation shows direct and indirect muscle attachments in wild-type (*E*) and *kak* mutant embryos (*F*). At indirect muscle attachments extracellular tendon matrix (*white arrowheads*) connects muscles to each other and to the epidermis (Prokop et al., 1998). Rupture of the epidermis at *kak* mutant indirect muscle attachments (*arrow* in *F*) allows muscles to remain connected to each other via tendon matrix but causes detachment from the epidermis (data not shown). Microtubules have been drawn to connect to dense material on the apical cell surface (Tepass and Hartenstein, 1994) although we are not certain about this fact in *kak* mutant embryos. Bars: (*A* and *B*) 1.5 μm; (*C* and *D*) 500 nm.

required for cytoskeletal organization. This is most obvious for muscle attachments to the epidermis. At stage 16 we could not detect any obvious defect in the muscle pattern of *kak* mutant embryos (*SF20/el3* and *91k/HG25*) (data not shown). However, at stage 17 the same alleles of *kak* cause severe detachment of muscles from the cuticle, but many muscles remain attached to each other (Fig. 6 *F*). Muscle attachments are formed by hemiadherens junctions, the adhesion of which depend on PS integrins (Fig. 6, *D* and *arrowheads* in *B*) (Tepass and Hartenstein, 1994; Prokop et al., 1998). In late stage 17 *kak* mutant embryos the extracellular adhesion of hemiadherens junctions is intact (Fig. 6, *C* and *arrowheads* in *A*) and, accordingly, β_{PS} integrin is expressed at the muscle tips (data not shown). However, we observe a striking phenotype on the intracellular face of hemiadherens junctions, only on the epidermal side. Normally the intracellular face of epidermal hemiadherens junctions contains a thick layer of electron-dense material, which connects to the stress-resisting microtubules (Fig. 6 *D*, *bent white arrow*). In *kak* mutant epidermal cells the layer of dense material is thinner (Fig. 6 *C*, *bent white arrow*) and microtubules, although present within the cell (Fig. 6, *open arrows*), seem not to be attached to the remaining layer of dense material. As a result, epidermal cells rupture (Fig. 6, *A* and *F*, *black arrows*), and the retracting muscles take with them the epidermal cell fraction around the hemiadherens junction. This phenotype is similar to BPAG1 mutant mice where intermediate filaments, the major stress-resisting cytoskeletal elements in epidermal cells of vertebrates, fail to adhere to hemidesmosomes (Guo et al., 1995).

Epidermal cells at sites of muscle attachments contain β1-tubulin, which is also strongly expressed throughout the central nervous system and in the scolopidia, which are part of the peripheral nervous system (also called chordotonal organs; Buttgereit et al., 1991). As growth defects in the nervous system are restricted to small dendrites and neuromuscular side branches, potential defects in their cytoskeleton are expected to be subtle, and so far we have not been able to pinpoint specific defects at the ultrastructural level. However, analysis of the more prominent scolopidia yielded interesting results. In the wild type, scolopidial sensory neurons form a long process stretched between cap and sheath cells and the soma bulges out asymmetrically on one side (Hartenstein, 1988; Carlson et al., 1997) (Fig. 7 *A*). The neuronal processes contain a typical ciliary apparatus with a cilium, basal body, and rootlet. The rootlets are surrounded by a circle of microtubules,

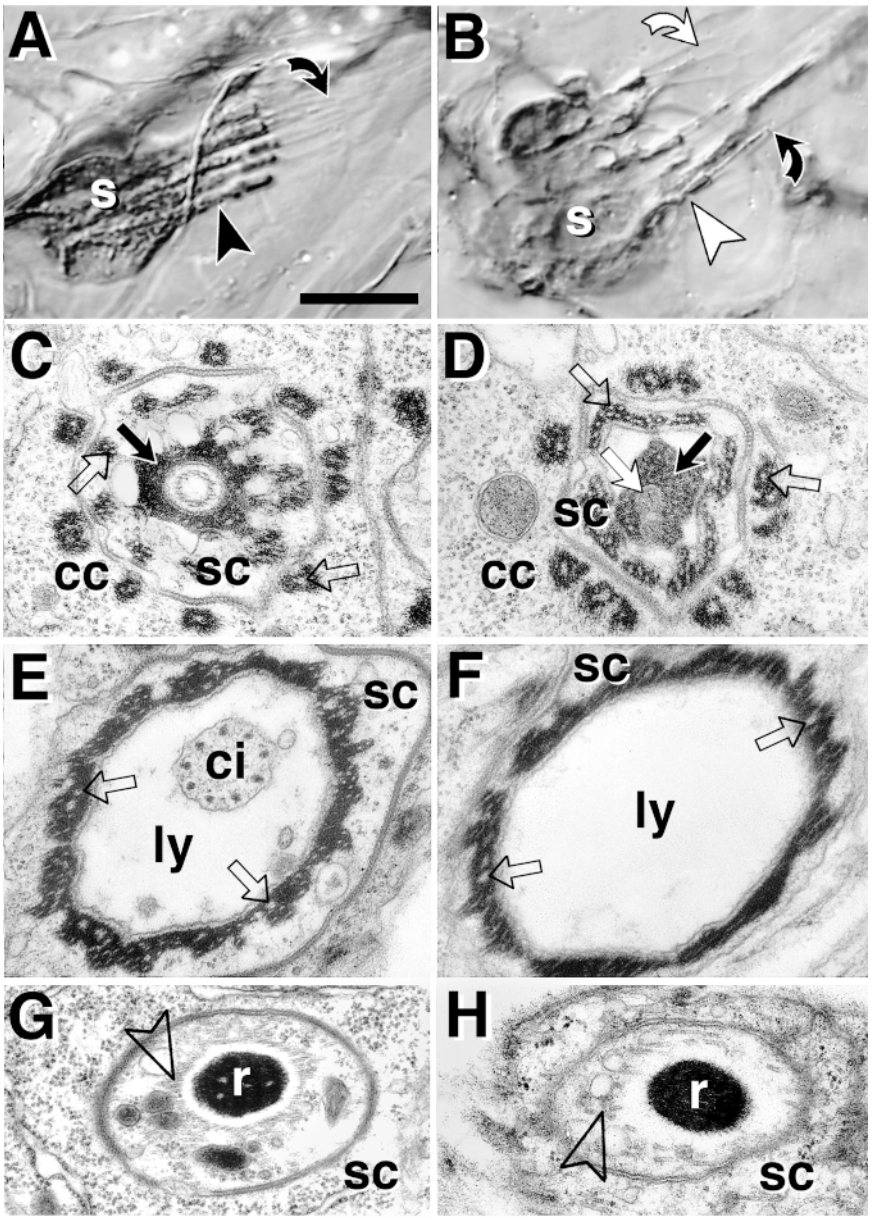

Figure 7. *kak* is required for the differentiation of scolopidial sensory neurons. All images are taken from late stage 17 embryos or freshly hatched larvae. Wild-type on the left, *kak* mutant scolopidia on the right. (*A* and *B*) Light microscope images of 22C10-labeled pentascolopidial organs (group of five scolopidia). (*A*) Cell bodies of scolopidial neurons (*s*) send out thick dendrites (*arrowhead*) extending into thin cilia, which have their ends attached to the tip of hollow lymph-filled capsules (*bent black arrow*). (*B*) In *kak* mutant scolopidia (tested alleles: *SF20/91k*, *SF20/el3*) the thick dendrites appear collapsed towards the somata (*white arrowheads*) and cilia frequently appear detached from the tip of the capsule (*bent white arrow*). (*C–H*) Ultrastructural phenotypes (tested alleles: *SF20/SF20*, *91k/91k*, *SF20/91k*). (*C*) At the tip of the capsule (*bent black arrow* in *A*), the cilium is anchored in extracellular matrix (*black arrow*) attached to the scolopale cell (*sc*) which is surrounded by processes of the cap cell (*cc*). (*D*) In *kak* mutant scolopidia grey inclusions (*white arrow*) can be found in the extracellular matrix, which might represent remnants of the cilium. (*E*) Further proximal the cilium (*ci*) is seen in the lymph-filled capsule (*ly*), surrounded by the scolopale cell. (*F*) The cilium is often missing at this position in *kak* mutant scolopidia. (*G*) Further proximal (*black arrowhead* in *A*) the dendrite contains the ciliary rootlet (*r*) surrounded by a circle of microtubules (*open arrowhead*). (*H*) *kak* mutant rootlets either lack a circle of microtubules or it is poorly developed. Intracellular dense material in cap and scolopale cells shows deeply embedded microtubules in control and mutant embryos (*white stipples*, *open arrows* in *C–F*). Note that microtubules are differently anchored at hemiadherens junctions, where they are not embedded in but associated with the dense material (Fig. 6 *D*). Bars: (*A* and *B*) 10 μm; (*C–H*) 480 nm.

especially in the distal parts of the processes. This circle of microtubules is mostly absent or very poorly developed in *kak* mutant embryos (Fig. 7, compare *G* with *H*), and the prominent dendrites appear collapsed in 22C10-labeled specimens (Fig. 7 *B*, *white arrowhead* and *white bent arrow*). The cilia contain a ring of nine microtubule doublets and are each located in a lymph-filled capsule formed by scolopale and cap cells (Fig. 7 *E*). The cilia are anchored with their apical ends in extracellular matrix at the tip of the capsules (Fig. 7 *C*). In *kak* mutant embryos the cilia look normal (data not shown), however, they fail to anchor at the capsule tips and are retracted (Fig. 7 *F*). In some mutant embryos we found grey inclusions within the extracellular matrix at the capsule tips, which might be remnants of the cilia (Fig. 7 *D*). This could suggest an intracellular detachment of the cilia similar to that seen in the epidermis, leaving behind pieces of fractured membrane.

Taken together, we could demonstrate defects in the cytoskeleton of two ectodermal tissues, suggesting that growth defects in the nervous system might have a similar cause. The synaptic phenotype, as well as the localization of kak-immunoreactivity at the NMJ, suggest that *kak* is required within the neuron (see Discussion). This interpretation is in good agreement with sequence data suggesting that *kak* codes for a cytoskeletal element with homologies to the actin-binding domain of plectin and BPAG1, the coiled-coil region of dystrophin, and parts of the GAS2 protein (Gregory and Brown, 1998; Strumpf and Volk, 1998).

Discussion

kak Mutations Specifically Affect Local Neuronal Growth

Growth of neuronal processes can be subdivided into (*a*) long-distance growth into target areas and (*b*) local growth within target areas. Here we describe the phenotypes of four independently isolated alleles of *kakapo* (kak^{SF20}, kak^{el3}, kak^{91k}, and kak^{HG25}), all of which show specific defects in local neuronal growth. In *kak* mutant embryos growth cones project into the correct target areas in the muscle field and in the neuropile but, subsequently, subsets of dendrites or NMJ branches fail to develop. Local dendritic growth in the neuropile is likely to be carried out by secondary growth cones budding off primary axons de novo (Tessier-Lavigne and Goodman, 1996). Branch formation at the NMJ takes place at about the same time as dendrite formation but occurs in a slightly different manner, in that the primary growth cone has already occupied space on the muscle but refines its shape into branches and boutons (Broadie and Bate, 1993; Yoshihara et al., 1997). The *kak* mutant phenotype strongly suggests that the final formation of both kinds of structures requires common molecular mechanisms.

The transition from long-distance growth to local branch formation appears to be a regulated process. It seems to be facilitated or accelerated by the function of the *late bloomer* gene, as loss of *late bloomer* function causes delay of NMJ differentiation after correct arrival of the growth cone (Kopczynski et al., 1996). One of the genes downstream in this pathway could be *kak*, since loss of *kak* function seems to cause growth defects after the growth cone arrives at the muscle. Loss of *kak* function leads to smaller NMJ branches and boutons, and the number of synapses and T-bars appears reduced. Also in *mbc*, *mef2* or *twist* mutant embryos NMJs are reduced or absent (caused indirectly by defects of the target muscles; Prokop et al., 1996), but the respective motorneurons still form varicosities and T-bars in fairly normal amounts, and T-bars which can't be placed apposed to muscle surfaces get localized at extrajunctional sites. In contrast, presynaptic specializations (presynaptic markers and T-bars) (Fig. 1) remain restricted to neuromuscular sites in *kak* mutant embryos, in spite of the fact that NMJs are severely reduced. We conclude that our *kak* mutant alleles might cause structural defects within the presynaptic terminals independently of target muscles. This interpretation is in agreement with cloning data demonstrating that *kak* encodes a cytoskeletal element with actin binding properties and a coiled coil region (Gregory and Brown, 1998; Strumpf and Volk, 1998). As kak is localized at the motorneuron terminal (Fig. 3) it might play a direct role in changes of the terminals' cytoskeleton which are required for growth and synapse formation.

kak Function Is Required for the Regulation of the Microtubule Cytoskeleton and Localization of Membrane Proteins

In addition to the growth defects in motorneurons, *kak* mutant embryos exhibit defects of the microtubule cytoskeleton in epidermal cells at muscle attachments and in scolopidial sensory neurons. The clearest phenotype is at muscle attachments, where the dense material associated with hemiadherens junctions on the basal side of the epidermis is reduced in thickness and fails to anchor microtubules. Thus, *kak* is required to mediate the link between the intracellular cytoskeleton and membrane-associated proteins. Thinning of the dense material at *kak* mutant hemiadherens junctions suggests that *kak* protein might be an integral part of the membrane-associated cytoskeleton, which would be in accordance with immunocytochemical localization of kakapo at the basal surface of muscle-attached epidermis cells (Gregory and Brown, 1998; Strumpf and Volk, 1998). If this interpretation is correct, kak could bind to the actin network underlying the membrane and link (indirectly) to microtubules, thus mediating attachment of microtubules to the membrane.

However, kak may not be restricted to specialized membrane areas like hemiadherens junctions. For example, dystrophin (in part homologous to *kak*) is concentrated at specialized junctions like synapses, but also found at nonspecialized membrane surfaces (Cartaud et al., 1992). If *kak* were similarly spread over neuronal surfaces it could regulate the localization of Fas II or 22C10 antigens (Fig. 5) by linking them to the underlying actin cytoskeleton. Loss of this kind of *kak* function might also cause the irregular appearance of the cell surfaces of dorsal bipolar dendrite neurons (Fig. 5 *K*) or the soma of RP3 (Fig. 4, *D* and *F*). Kak may even be localized in the cytoplasm, like its partial homologue BPAG1, which is localized in membrane-associated dense material of epidermal hemidesmosomes, but in the cytoplasm of neurons (in another splice version; Fuchs and Cleveland, 1998). Similarly, the organization of microtubules in scolopidial sensory neurons (Fig. 7 *H*) might require *kak* function within the cytoplasm where kak could link microtubules to the actin network or to the ciliary rootlet. Alternatively the defect of microtubules in scolopidial neurons could be caused secondarily due to loss of *kak*-mediated anchoring at the dendrite tip, comparable to the phenotype at epidermal hemiadherens junctions. The latter possibility is supported by the finding that kak is localized at the dendrite tip of scolopidial neurons (Gregory and Brown, 1998). Interestingly, our staining procedure failed to detect kak staining in the epidermis or scolopidial organs at stage 16, 17 or in the late larva. This might hint at different splice versions of kak or at a different molecular context.

Possible Causes for Defects in Local Sprouting

We have demonstrated two different defects at the subcellular level in *kak* mutant embryos. First, the localization of axonal proteins is affected and, secondly, there are defects in the microtubule organization of some cell types. Both defects may be the underlying cause for the observed reduction in local growth of dendrites and at NMJs.

It has been shown that branching of motorneuronal terminals and axonal defasciculation require a reduction of neuronal cell adhesion molecule (N-CAM)-mediated interaxonal adhesion in vertebrates (Landmesser et al., 1990) and, in agreement with this, overexpression of Fas II, the *Drosophila* homologue of N-CAM, antagonizes nerve branching (Lin et al., 1994). Hence, we reasoned

that the inhibition of dendrite and branch formation might be due to the observed mislocalization of Fas II to axonal areas where dendrites and terminal branches are usually forming. However, combining *kak* with the *Fas II*^{eb112} null allele (Grenningloh et al., 1991) did not show any obvious suppression of the neuromuscular phenotype (data not shown). Thus, mislocalization of Fas II alone does not explain the growth defects, but its involvement might be obscured by mislocalization of other redundant CAMs of similar function (Speicher et al., 1998). Mislocalization of membrane proteins might be the consequence of their lack of a *kak*-mediated linkage to the membrane-associated cytoskeleton (see above). Conversely, loss of such a physical link could cause disruption of growth regulation, as transmembrane proteins have been shown to instruct the assembly of the actin cytoskeleton in neuronal growth cones (Thompson et al., 1996; Suter and Forscher, 1998).

Neuronal growth defects in *kak* mutant embryos might be caused directly by defects in cytoskeleton assembly. Microtubules are essential for axonal growth and are regulated in a complex way. For example, low concentrations of taxol do not interfere with growth cone advance in general, but render growth cones unable to turn when they come into contact with a repellent signal (Challacombe et al., 1997). The assembly of microtubules during growth is preceded by formation of the actin cytoskeleton. Accordingly, growth cone turning can be blocked upon low application of cytochalasin-B, indicating cooperation between the actin and tubulin cytoskeleton in this specific growth event (Challacombe et al., 1996). The fine regulation of microtubules has been shown to require MAPs (Avila et al., 1994). Similarly, the fine regulation of actin could require actin-associated proteins, and kak might be one of them. This might explain why loss of *kak* function suppresses only a specific subset of neuronal growth events, i.e., local growth at NMJs and of contralateral RP3 dendrites but not long distance growth or ipsilateral RP3 arbors. The specific growth defects in *kak* mutant embryos might be due to subcellular-specific compartmentalization of *kak* or local posttranslational modifications, as has similarly been demonstrated for MAPs (Avila et al., 1994). Alternatively, unaffected branches may contain redundant cytoskeletal molecules that the affected branches lack. Possible molecular differences might reflect a general difference between affected and unaffected branches. For example, affected branches might represent preferentially presynaptic output branches (certainly true for NMJs) and unaffected branches may represent postsynaptic or input branches. Alternatively, the qualitative differences might consist in the origin of the branches: arborizations derived from an axon (NMJ, contralateral RP3 dendrites) may require *kak* function, but not those derived from somatic extensions (ipsilateral RP3 dendrites).

We are grateful to M. Ashburner (University of Cambridge, Cambridge, UK), in whose laboratory the mutageneses were carried out, to H. Bellen (Baylor College of Medicine, Howard Hughes Medical Institute [HHMI], Houston, TX), M. González-Gaitán (Max Planck Institute for Biophysical Chemistry, Göttingen, Germany), C.S. Goodman (University of California, HHMI, Berkeley, CA), and K. Zinsmaier (University of Pennsylvania School of Medicine, Philadelphia, PA) for providing antibodies, to C. Schuster (Max Planck Institute) for providing flies, to N. Brown, S. Gregory (both from University of Cambridge, Wellcome Institute), D. Strumpf, and T. Volk (both from Weizmann Institute, Rehovot, Israel) for helpful exchange of information and fly stocks and generously sending anti-kakapo antisera. We would like to thank R. Baines, M. Landgraf, and N. Sánchez-Soriano (all three from University of Cambridge) for critical comments on the manuscript and S.D. Carlson for comments on Figure 7. J. Uhler would like to thank A. Sossick and A. Brand (both from University of Cambridge, Wellcome Institute) for help and advice on confocal microscopy. A. Prokop is grateful to R. Baines for teaching and advising on the patch-clamp technique and to K. Broadie (University of Utah, Salt Lake City, UT) for additional advice, to G. Technau in whose laboratory part of the work was carried out, and to E. Sehn and G. Eisenbeis (all three from University of Mainz, Mainz, Germany) for advice and help on the Hitachi microscope.

M. Bate was funded by a grant from the Wellcome Trust (052032/Z/97/Z), A. Prokop by a research fellowship from the Lloyd's of London Tercentenery Foundation (LTF/GL/FEL95), and J. Uhler by a grant from the Overseas Research Students Awards Scheme.

Received for publication 24 April 1998 and in revised form 14 September 1998.

References

Angau-Petit, D., P. Toth, O. Rogero, L. Faille, F.J. Tejedor, and A. Ferrús. 1998. Enhanced neurotransmitter release is associated with reduction of neuronal branching in a *Drosophila* mutant overexpressing frequenin. *Eur. J. Neurosci.* 10:423–434.

Arcaro, K.F., and G.A. Lnenicka. 1995. Intrinsic differences in axonal growth from crayfish fast and slow motorneurons. *Dev. Biol.* 168:272–283.

Ashburner, M., J. Faithfull, T. Littlewood, G. Richards, S. Smith, V. Velissariou, and R.C. Woodruff. 1980. Report of new mutants—*Drosophila melanogaster*. *Dros. Info. Service.* 55:193–195.

Avila, J., J. Domínguez, and J. Díaz-Nido. 1994. Regulation of microtubule dynamics by microtubule-associated protein expression and phosphorylation during neuronal development. *Int. J. Dev. Biol.* 38:13–25.

Bate, M. 1993. The mesoderm and its derivatives. *In* The Development of *Drosophila melanogaster*. M. Bate and A. Martínez Arias, editors. Cold Spring Harbor Laboratory Press, Cold Spring Harbor, NY. 1013–1090.

Bate, M., and K. Broadie. 1995. Wiring by fly: the neuromuscular system of the *Drosophila* embryo. *Neuron*. 15:513–525.

Bentley, D., and T.P. O'Connor. 1994. Cytoskeletal events in growth cone steering. *Curr. Opin. Neurobiol.* 4:43–48.

Bodmer, R., and Y.N. Jan. 1987. Morphological differentiation of the embryonic peripheral neurons in *Drosophila*. *Roux's Arch. Dev. Biol.* 196:69–77.

Broadie, K., A. Prokop, H.J. Bellen, C.J. O'Kane, K.L. Schulze, and S.T. Sweeney. 1995. Syntaxin or synaptobrevin function downstream of vesicle docking in *Drosophila*. *Neuron.* 15:663–673.

Broadie, K.S., and M. Bate. 1993. Development of the embryonic neuromuscular synapse of *Drosophila melanogaster*. *J. Neurosci.* 13:144–166.

Buttgereit, D., D. Leiss, F. Michiels, and R. Renkawitz-Pohl. 1991. During *Drosophila* embryogenesis the β1 tubulin gene is specifically expressed in the nervous system and the apodemes. *Mech. Dev.* 33:107–118.

Caceres, A., J. Mautino, and K.S. Kosik. 1992. Suppression of MAP2 in cultured cerebellar macroneurons inhibits minor neurite formation. *Neuron.* 9:607–618.

Caceres, A., S. Potrebic, and K.S. Kosik. 1991. The effect of tau antisense oligonucleotides on neurite formation of cultured cerebellar macroneurons. *J. Neurosci.* 11:1515–1523.

Canal, I., A. Acebes, and A. Ferrús. 1998. Single neuron mosaics of the *Drosophila gigas* mutant project beyond normal targets and modify behaviour. *J. Neurosci.* 18:999–1008.

Carlson, S.D., S.L. Hilgers, and J.L. Juang. 1997. Ultrastructure and blood-nerve barrier of chordotonal organs in the *Drosophila* embryo. *J. Neurocytol.* 26:377–388.

Caroni, P. 1997. Intrinsic neuronal determinants that promote axonal sprouting and elongation. *Bioessays.* 19:767–775.

Cartaud, A., M.A. Ludosky, F.S. Tomé, H. Collin, F. Stetzkowski-Marden, T.S. Khurana, L.M. Kunkel, M. Fardeau, J.P. Changeux, and J. Cartaud. 1992. Localisation of dystrophin and dystrophin-related protein at the electromotor synapse and neuromuscular junction in Torpedo marmorata. *Neuroscience.* 48:995–1003.

Challacombe, J.F.S., D.M. Snow, and P.C. Letourneau. 1996. Actin filament bundles are required for microtubule reorientation during growth cone turning to avoid an inhibitory guidance cue. *J. Cell Sci.* 109:2031–2040.

Challacombe, J.F., D.M. Snow, and P.C. Letourneau. 1997. Dynamic microtubule ends are required for growth cone turning to avoid an inhibitory guidance cue. *J. Neurosci.* 17:3085–3095.

Dinsmore, J., and F. Solomon. 1991. Inhibition of MAP-2 expression affects both morphological and cell division phenotypes of neuronal differentiation. *Neuron.* 9:607–618.

Eberl, D.F., A.J. Hilliker, C.B. Sharp, and S.N. Trusis-Coulter. 1989. Further observations on the nature of radiation-induced chromosomal interchanges recovered from *Drosophila* sperm. *Genome.* 32:847–855.

Fuchs, E., and D.W. Cleveland. 1998. A structural scaffolding of intermediate filaments in health and disease. *Science.* 279:514–519.

Fujita, S.C., S.L. Zipursky, S. Benzer, A. Ferrús, and S.L. Shotwell. 1982. Monoclonal antibodies against the *Drosophila* nervous system. *Proc. Natl. Acad. Sci. USA.* 79:7929–7933.

González-Gaitán, M., and H. Jäckle. 1997. Role of Drosophila α-adaptin in presynaptic vesicle recycling. *Cell.* 88:767–776.

Goodman, C.S., and C.Q. Doe. 1993. Embryonic development of the *Drosophila* central nervous system. *In* The Development of *Drosophila melanogaster.* M. Bate and A. Martínez Arias, editors. Cold Spring Harbor Laboratory Press, Cold Spring Harbor, NY. 1131–1206.

Gregory, S.L., and N.H. Brown. 1998. *kakapo*, a gene required for adhesion between cell layers in *Drosophila*, encodes a large cytoskeletal linker protein related to plectin and dystrophin. *J. Cell Biol.* 143:1271–1282.

Grenningloh, G., E.J. Rehm, and C.S. Goodman. 1991. Genetic analysis of growth cone guidance in *Drosophila*: fasciclin II functions as a neuronal recognition molecule. *Cell.* 67:45–57.

Guo, L., L. Degenstein, J. Dowling, Q.-C. Yu, R. Wollmann, B. Perman and E. Fuchs. 1995. Gene targeting of BPAG1: abnormalities in mechanical strength and cell migration in stratified squamous epithelia and severe neurologic degeneration. *Cell.* 81:233–243.

Halpern, M.E., A. Chiba, J. Johansen, and H. Keshishian, H. 1991. Growth cone behaviour underlying the development of stereotypic synaptic connections in *Drosophila* embryos. *J. Neurosci.* 11:3227–3238.

Hartenstein, V. 1988. Development of *Drosophila* larval sensory organs: spatiotemporal pattern of sensory neurons, peripheral axonal pathways and sensilla differentiation. *Development (Camb.).* 102:869–886.

Kopczynski, C.C., D.W. Davis, and C.S. Goodman. 1996. A neural tetraspanin, encoded by late bloomer, that facilitates synapse formation. *Science.* 271: 1876–1870.

Landgraf, M., T. Bossing, G.M. Technau, and M. Bate. 1997. The origin, location, and projection of the embryonic abdominal motorneurons of *Drosophila. J. Neurosci.* 17:9642–9655.

Landmesser, L., L. Dahm, J. Tang, and U. Rutishauser. 1990. Polysialic acid as a regulator of intramuscular nerve branching during embryonic development. *Neuron.* 4:655–667.

Lin, D.M., R.D. Fetter, C. Kopczynski, G. Grenningloh, and C.S. Goodman. 1994. Genetic analysis of fasciclin II in *Drosophila*: defasciculation, refasciculation, and altered fasciculation. *Neuron.* 13:1055–1069.

Littleton, J.T., H.J. Bellen, and M.S. Perin. 1993. Expression of synaptotagmin in *Drosophila* reveals transport and localization of synaptic vesicles in the synapse. *Development (Camb.).* 118:1077–1088.

Murphey, R.K., and C.A. Lemere. 1984. Competition controls the growth of an identified axonal arborization. *Science.* 224:1352–1355.

Nobes, C.D., and A. Hall. 1995. Rho, Rac, Cdc42 GTPases regulate the assembly of multimolecular focal complexes associated with actin stress fibers, lamellipodia, and filopodia. *Cell.* 81:53–62.

Preston, C.R., J.A. Sved, and W.R. Engels. 1996. Flanking duplications and deletions associated with P-induced male recombination in *Drosophila. Genetics.* 144:1623–1638.

Prokop, A., M. Landgraf, E. Rushton, K. Broadie, and M. Bate. 1996. Presynaptic development at the *Drosophila* neuromuscular junction: the assembly and localisation of presynaptic active zones. *Neuron.* 17:617–626.

Prokop, A., M.D. Martín-Bermudo, M. Bate, and N. Brown. 1998. Absence of PS integrins or laminin A affects extracellular adhesion, but not intracellular assembly, of hemiadherens and neuromuscular junctions in *Drosophila* embryos. *Dev. Biol.* 196:58–76.

Prokop, A., and G.M. Technau. 1993. Cell transplantation. *In* Cellular Interactions in Development: A Practical Approach. D. Hartley, editor. Oxford University Press, London, UK. 33–57.

Prout, M., Z. Damania, J. Soong, D. Fristrom, and J.W. Fristrom. 1997. Autosomal mutations affecting adhesion between wing surfaces in *Drosophila melanogaster. Genetics.* 146:275–285.

Reddy, S., P. Jin, J. Trimarchi, P. Caruccio, R. Phillis, and R.K. Murphey. 1997. Mutant molecular motors disrupt neural circuits in *Drosophila. J. Neurobiol.* 33:711–723.

Ruegg, M.A., and J.L. Bixby. 1998. Agrin orchestrates synaptic differentiation at the vertebrate neuromuscular junction. *Trends Neurosci.* 21:22–27.

Sink, H., and P.M. Whitington. 1991. Pathfinding in the central nervous system and periphery by identified embryonic *Drosophila* motor axons. *Development (Camb.).* 112:307–316.

Smith, C.L. 1994. Cytoskeletal movements and substrate interactions during initiation of neurite outgrowth by sympathetic neurons in vitro. *J. Neurosci.* 14:384–398.

Speicher, S., L. Garcia-Alonso, A. Carmena, M.D. Martín-Bermudo, S. de la Escalera, and F. Jiménez. 1998. Neurotactin functions in concert with other identified CAMs in growth cone guidance in *Drosophila. Neuron.* 20:221–233.

Strumpf, D., and T. Volk. 1998. Kakapo, a novel *Drosophila* protein, is essential for the restricted localization of the neuregulin-like factor, Vein, at the muscle–tendon junctional site. *J. Cell Biol*. 143:1259–1270.

Suter, D.M., and P. Forscher. 1998. An emerging link between cytoskeletal dynamics and cell adhesion molecules in growth cone guidance. *Curr. Opin. Neurobiol.* 8:106–116.

Tepass, U., and V. Hartenstein. 1994. The development of cellular junctions in the *Drosophila* embryo. *Dev. Biol.* 161:563–596.

Tessier-Lavigne, M., and C.S. Goodman. 1996. The molecular biology of axon guidance. *Science.* 274:1123–1133.

Thomas, J.B., M.J. Bastiani, M. Bate, and C.S. Goodman. 1984. From grasshopper to *Drosophila*: a common plan for neural development. *Nature.* 310:203–206.

Thompson, C., C.-H. Lin, and P. Forscher. 1996. An *Aplysia* cell adhesion molecule associated with site-directed actin filament assembly in neuronal growth cones. *J. Cell Sci.* 109:2843–2854.

Van Vactor, D., H. Sink, D. Fambrough, R. Tsoo, and C.S. Goodman. 1993. Genes that control neuromuscular specificity in *Drosophila. Cell.* 73:1137–1153.

Yoshihara, M., M.B. Rheuben, and Y. Kidokoro. 1997. Transition from growth cone to functional motor nerve terminal in *Drosophila* embryo. *J. Neurosci.* 17:8408–8426.

Zinsmaier, K.E., K.K. Eberle, E. Buchner, N. Walter, and S. Benzer. 1994. Paralysis and early death in cysteine string protein mutants of *Drosophila. Science.* 263:977–980.